van der Waals bonding and the quasiparticle band structure of SnO from first principles

Kirsten Govaerts,[1,*] Rolando Saniz,[2] Bart Partoens,[2] and Dirk Lamoen[1]
[1]*EMAT, Universiteit Antwerpen, Groenenborgerlaan 171, 2020 Antwerpen, Belgium*
[2]*CMT group, Department of Physics, Universiteit Antwerpen, Groenenborgerlaan 171, 2020 Antwerpen, Belgium*
(Received 8 March 2013; revised manuscript received 11 June 2013; published 28 June 2013)

In this work we have investigated the structural and electronic properties of SnO, which is built up from layers kept together by van der Waals (vdW) forces. The combination of a vdW functional within density functional theory (DFT) and quasiparticle band structure calculations within the GW approximation provides accurate values for the lattice parameters, atomic positions, and the electronic band structure including the fundamental (indirect) and the optical (direct) band gap without the need of experimental or empirical input. A systematic comparison is made between different levels of self-consistency within the GW approach {following the scheme of Shishkin *et al.* [Phys. Rev. B **75**, 235102 (2007)]} and the results are compared with DFT and hybrid functional results. Furthermore, the effect of the vdW-corrected functional as a starting point for the GW calculation of the band gap has been investigated. Finally, we studied the effect of the vdW functional on the electron charge density.

DOI: 10.1103/PhysRevB.87.235210 PACS number(s): 71.20.Nr, 71.15.Mb, 31.15.ac, 31.15.ae

I. INTRODUCTION

Both SnO_2 and SnO show a wide variety of technological applications. Whereas the former acts as a functional material for solar cells,[1] transparent conducting oxides,[2,3] and gas sensors,[4] the latter is used for the production of tin salts for electroplating[5] and is known as an anode material for Li-rechargeable batteries.[6] Moreover, SnO is a good p-type semiconductor,[7] which can even be converted from p to n type after doping with Sb.[8]

The most stable form of SnO is the so-called litharge form which has a tetragonal structure (space group $P4/nmm$) with lattice parameters $a = 3.801$ Å and $c = 4.835$ Å.[9] The oxygen atoms form the base of a square pyramid with the tin atom located at the apex, resulting in a layered stacking of Sn-O-Sn slabs along the [001] direction with each slab consisting of an oxygen layer sandwiched between two tin layers as shown in Fig. 1. The oxygen atoms are located at positions (0,0,0) and (0.5,0.5,0) and the position of the tin atoms is given by $(0,0.5,u)$ and $(0.5,0,-u)$ with $u = 0.2381$.[9] Between the Sn-O-Sn slabs, i.e., between adjacent Sn layers, a weak van der Waals (vdW) bonding exists with a distance of 2.53 Å between successive slabs. The structural and electronic properties of SnO have been studied far less with first-principles computational techniques than those of SnO_2. In particular, density functional theory (DFT) was used successfully in a series of papers[10–13] to clarify the relation between the structural (and electronic) properties and the nature of the so-called lone pair electrons. As expected, all DFT results underestimate the fundamental and optical band gap. The fundamental band gap is found experimentally to be indirect with a value of ∼0.7 eV, while the direct optical gap has a value of ∼2.7 eV.[7,14] DFT results for the (fundamental) band gap vary between no gap and 0.6 eV,[10,15–20] depending strongly on the used exchange and correlation (xc) functional, basis set, and lattice parameters (computationally optimized versus experimental values). For example, using the experimental lattice parameters, a full-potential linearized-augmented-plane-wave calculation[21] gives a value of 0.3 eV for the band gap with both the local density and generalized gradient approximation (LDA and GGA, respectively) for the xc functional, whereas other results are often much closer to the experimental value.[10,19,20] All these results can be rationalized by noticing that the band gap depends sensitively on the total volume, thereby yielding larger band gaps with increasing volume.[22] In contrast to many other semiconductors and insulators, the band gap of SnO does not only suffer from the DFT discontinuity in the xc functional,[23] but also from the inability of traditional functionals to correctly describe the vdW bonding. In recent work an empirical vdW correction within the DFT approach was included to obtain structural parameters for SnO in line with experiment.[18,19] However, a more general approach to account for London dispersion forces within DFT is given by nonlocal correlation functionals and in particular the functional form proposed by Dion *et al.*:[24]

$$E_{\mathrm{xc}} = E_x^{\mathrm{GGA}} + E_c^{\mathrm{LDA}} + E_c^{nl},$$

where the exchange energy E_x^{GGA} is given by the generalized gradient approximation (GGA) and the correlation energy has a local part E_c^{LDA}, given by the local density approximation (LDA), and a nonlocal part E_c^{nl}, which accounts approximately for the nonlocal electron correlation effects. Using the efficient implementation of the vdW functional by Román-Pérez and Soler[25] a self-consistent calculation[26] takes hardly more time than a standard GGA calculation.

In the first part of this work a comparison between several versions of nonlocal correlation functionals as discussed in Ref. 27 is presented. We show that the so-called optB86b van der Waals density functional (vdW-DF) yields structural parameters for SnO in very good agreement with experiment. Using this structure we find a reliable band gap from quasiparticle band structure calculations within the GW approximation[28] as implemented[29,30] in the VASP code.[31,32] In fact, we will consider three levels of sophistication: (i) Kohn-Sham eigenvalues and eigenfunctions are used to compute the Green's function G and the screened Coulomb interaction W (G_0W_0), (ii) updating the eigenvalues in the Green's function G (GW_0), and (iii) updating the eigenvalues in G and W (GW) (the latter will often be referred to as the self-consistent GW). Since the GW method is a perturbative approach the results depend on the choice of the xc functional

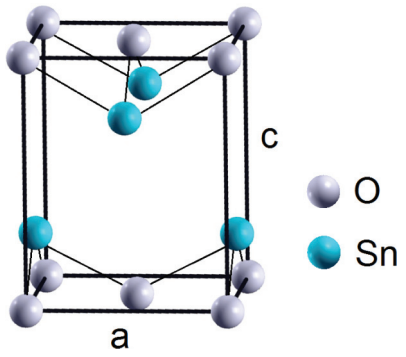

FIG. 1. (Color online) Unit cell.

used in the initial DFT calculation. Therefore we consider both vdW corrected and noncorrected functionals as input for the GW calculations. We also compare the GW results with those obtained from a hybrid functional approach using the HSE03 and HSE06 functionals.[33–37] Finally, we show the effect of the vdW DF on the charge density around the Sn and O atoms.

II. COMPUTATIONAL DETAILS

Optimized lattice parameters and atomic positions were obtained from relaxing the tetragonal SnO structure by using first-principles calculations performed within the DFT formalism as implemented in the Vienna *ab initio* simulation package VASP.[31,32] We used the all-electron projector augmented wave (PAW) method with the Sn ($5s^2 5p^2 4d^{10}$) and O ($2s^2 2p^2$) electrons treated as valence electrons. For the xc functional we considered both the generalized gradient approximation of Perdew-Burke-Ernzerhof (PBE)[38] and the vdW-DFs discussed in Ref. 27. In the remainder of the paper the different vdW-DFs will be denoted by the acronym given in Ref. 27.

For total energy calculations and structure optimization we used a $8 \times 8 \times 8$ grid for the Brillouin zone integration. The plane wave cutoff value was chosen 900 eV, so that our results are converged within 10^{-4} eV/atom. Both lattice parameters and atom coordinates are relaxed. For the electronic structure calculation we considered the results as converged when the energy difference between two successive steps was smaller than 10^{-5} eV and for the geometry optimization we considered a convergence criterium for the forces on the atoms of less than 10^{-3} eV/Å.

For the GW calculations, convergence is also carefully checked. We used a $6 \times 6 \times 6$ k-point grid and a cutoff energy of 600 eV. A thousand bands had to be included, and for the update of G and W, four steps are necessary to find band gap energies converged up to 10^{-3} eV.

For comparison band gaps have also been calculated with the hybrid functional proposed by Heyd, Scuseria, and Ernzerhof (HSE).[33] We consider both the original screening parameter $\mu = 0.3$ Å^{-1} (HSE03)[34] and $\mu = 0.2$ Å^{-1} (HSE06).[37]

III. RESULTS AND DISCUSSION

A. Structural properties

We relaxed the SnO structure—both lattice parameters and atomic positions—with the settings described in the previous section, by making use of different vdW-DFs implemented in VASP,[24,27,39] for which the results are shown in Table I. For comparison we added the bare PBE values without any vdW correction and those obtained from the empirical vdW correction suggested by Grimme.[40] Bare PBE overestimates the lattice parameters and in particular the distance between adjacent Sn layers is too large. Both optPBE-vdW and optB88-vdW functionals provide results similar to those of bare PBE, whereas the results for optB86b-vdW and the Grimme correction are much closer to experiment. In line with previous results[27,41] both the rPW86-vdW and revPBE-vdW functional give lattice constants that are too large. For completeness we also added to Table I the results obtained from hybrid functionals HSE03 and HSE06. Both hybrid functionals provide values for a and c closer to experiment than bare PBE. From Table I we conclude that both the Grimme potential and optB86b-vdW provide structural parameters in very good agreement with experiment, in particular for the distance between adjacent Sn layers, which depends strongly on the vdW forces. The structure optimization with the optB86b-vdW functional yields a nearest neighbor distance between Sn

TABLE I. Lattice parameters a and c (in Å), c/a ratio and internal coordinate u, optimized by making (no) use of the empirical vdW correction of Grimme,[40] the different vdW functionals described in Ref. 27, and two hybrid functionals. The interlayer distance (in Å) between adjacent Sn layers is also shown. The last column displays the total volume of the unit cell (in Å^3). Percentage changes with respect to the experimental values are given in parentheses.

	a	c	u	Sn-Sn	V
PBE	3.866(1.71)	5.032(4.07)	0.2312(−2.90)	2.705(6.82)	75.208(7.66)
Grimme	3.841(1.05)	4.831(−0.08)	0.2425(1.85)	2.488(−1.76)	71.273(2.03)
optB86b-vdW	3.840(1.03)	4.812(−0.48)	0.2411(1.26)	2.492(−1.62)	70.923(1.53)
optB88-vdW	3.862(1.60)	4.936(2.09)	0.2354(−1.13)	2.612(3.14)	73.621(5.39)
optPBE-vdW	3.881(2.10)	5.051(4.47)	0.2309(−3.02)	2.718(7.34)	76.079(8.91)
rPW86-vdW	3.961(4.21)	5.492(13.59)	0.2146(−9.87)	3.135(23.78)	86.167(23.35)
revPBE-vdW	3.924(3.24)	5.393(11.54)	0.2175(−8.65)	3.047(20.31)	83.040(18.88)
HSE03	3.804(0.08)	4.938(2.13)	0.2327(−2.27)	2.640(4.24)	71.455(2.29)
HSE06	3.800(−0.03)	4.960(2.59)	0.2319(−2.60)	2.660(5.01)	71.622(2.53)
Experiment	3.801	4.835	0.2381	2.533	69.854

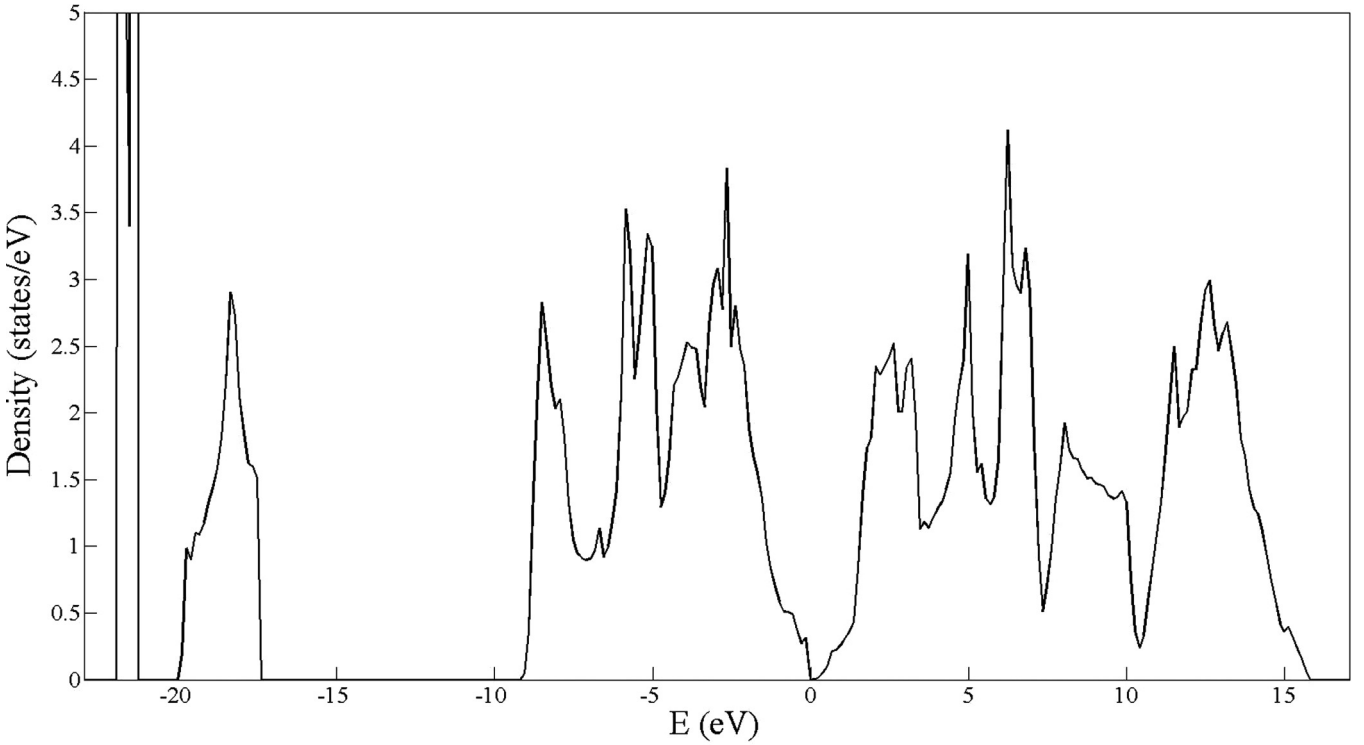

FIG. 2. The total density of states. Energy values are with respect to the top of the valence band.

and O of 2.243 Å, which is better than any other vdW-DF listed in Table I and in line with the experimental value of 2.222 Å. In the remainder of this paper we continue to work with the lattice parameters and atomic positions obtained with optB86b-vdW.

B. Electronic properties

In Fig. 2 the total density of states (DOS) calculated with optB86b-vdW (for a structure optimized with optB86b-vdW) is shown, for which a small band gap of 0.16 eV is observed. The partial DOS in Fig. 3 shows low energy contributions of

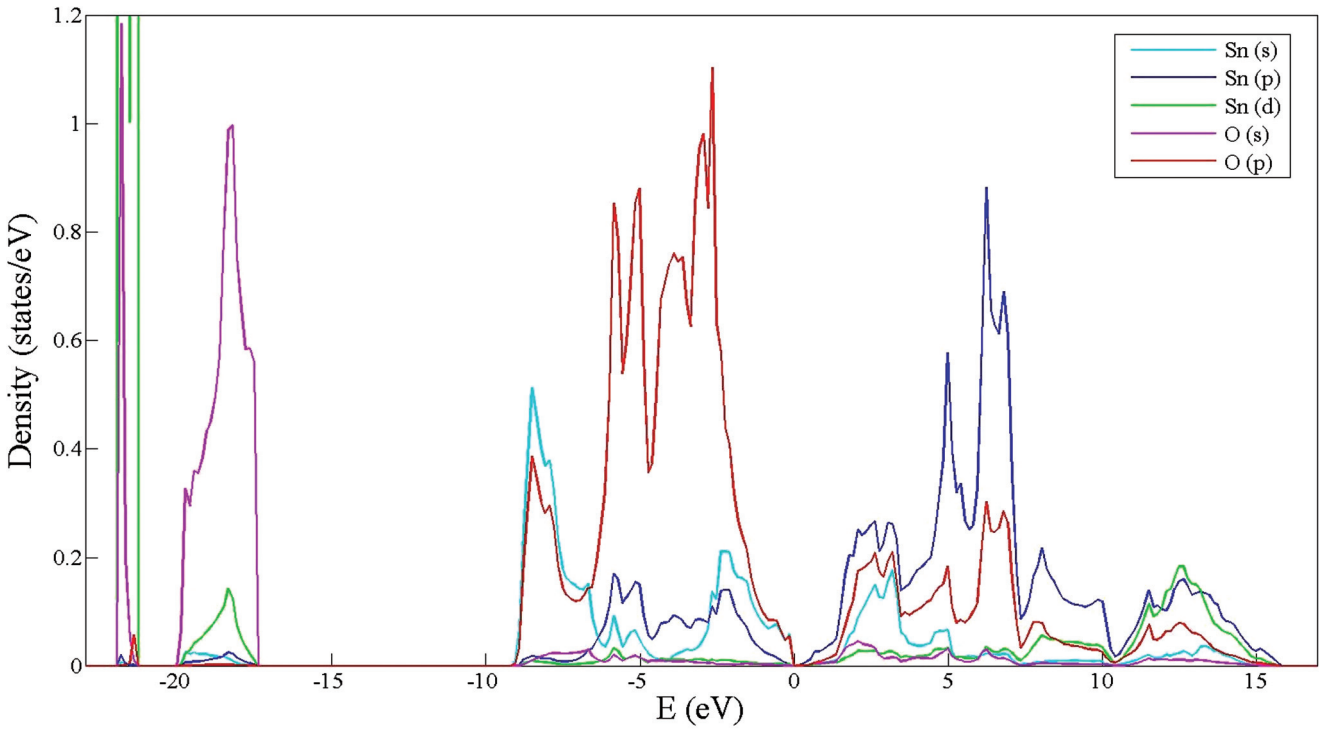

FIG. 3. (Color online) The projected density of states.

TABLE II. Indirect band gap (eV) for different lattice parameters, calculated with different methods.

Lattice parameters	Eigenfunctions	PBE	G_0W_0	GW_0	GW	HSE03	HSE06
Relaxed with PBE	PBE	0.43	1.09	1.22	1.40	0.69	0.84
	optB86b-vdW	0.50	1.14	1.27	1.45	–	–
Relaxed with optB86b-vdW	PBE	0.07	0.60	0.75	0.90	0.23	0.40
	optB86b-vdW	0.16	0.71	0.78	0.93	–	–
Experiment	PBE	0.04	0.53	0.71	0.86	0.22	0.36
	optB86b-vdW	0.13	0.67	0.78	0.94	–	–

the d electrons of Sn and the s electrons of O between -22.0 and -21.0 eV and -20.0 and -17.0 eV, respectively (with respect to the top of the valence band). The valence region can be divided into three regions: A region between -9.0 and -6.0 eV, consisting mainly of Sn s and O p electrons, a second region between -6.0 and -3.0 eV, in which the O p electrons play the most important role, with a small mixing with Sn p electrons and an even smaller contribution of Sn s electrons. In the third region, close to the valence band maximum, between -3.0 and 0 eV, the contribution is a mixing of O p, Sn s, and Sn p electrons, while at the maximum itself, only O p and Sn s electrons play a role. The conduction band is derived from Sn p, O p, and Sn s electrons, with the first giving the largest and the latter giving the smallest contribution. The conduction band minimum consists mainly of Sn p electrons. These findings are all in agreement with previous studies.[10–12,16,18,20,21,42]

In Table II we summarize our results for the fundamental band gap calculated with different approximations. We considered three structural models for SnO. For the first one (referred to as "relaxed with PBE" in Table II) the lattice parameters and atomic positions are optimized with the PBE functional excluding any vdW correction. The second model results from the optimization with the optB86b-vdW functional (referred to as "relaxed with optB86b-vdW") and the third one uses the experimental crystal structure (referred to as "experiment"). For a fixed structure we have solved the Kohn-Sham equations self-consistently for all three models with the bare PBE functional and the optB86b-vdW functional. The resulting eigenvalues and eigenfunctions were subsequently used as input for the GW calculations.

In all cases that have been studied, an indirect band gap was found between the Γ and M point. When the SnO structure is relaxed without vdW correction a value of 0.43 eV was found with the bare PBE functional. Although this result is not too far away from the experimental band gap of 0.7 eV, it is an artifact and a consequence of the failure of PBE to account for the vdW forces which results in a volume of 75.21 Å^3, while experiment gives 69.85 Å^3. This is in line with the strong dependence of the band gap with the volume.[22]

Furthermore, the well-known underestimation of the band gap by PBE (with or without vdW correction to the xc functional) is clearly demonstrated by the results listed in the first column of Table II. In particular for the vdW-relaxed and the experimental structures the band gap becomes very small. It should also be noticed that there is a systematic opening of the band gap when the vdW functional is used for the self-consistent calculation of the eigenvalues and eigenfunctions.

Although DFT eigenvalues do not provide accurate values for the band gap of semiconductors and insulators, they are still a good starting point for the quasiparticle calculations within the GW approximation. In Table II we list the results for the considered three levels of approximation (G_0W_0, GW_0, and GW) as explained in the Introduction. We clearly observe that for the structure optimized without vdW all GW results overestimate the band gap. But for the vdW relaxed and the experimental structure the GW calculations are already much better. In particular we obtain values close to experiment for G_0W_0 and GW_0. Updating both G and W self-consistently leads to an overestimation of the gap. Our results are in line with previous observations for small and large band gap semiconductors[30]: While G_0W_0 underestimates and GW overestimates the band gap, GW_0 provides good agreement with experiment. Our results are also in agreement with the 0.74 eV obtained in a recent G_0W_0 calculation based on the experimental crystal structure and using DFT-LDA eigenvalues and eigenfunctions as starting value.[43] The LDA

TABLE III. Direct band gaps (eV) for different lattice parameters, calculated with different methods. For the structure optimized with bare PBE, the gap is located at the Γ point, while for the vdW-optimized structure and the experimental lattice parameters, the gap is located at the M point.

Lattice parameters	Eigenfunctions	PBE	G_0W_0	GW_0	GW	HSE03	HSE06	
Relaxed with PBE	PBE	1.93	2.78	2.94	3.15	2.45	2.62	(Γ)
	optB86b-vdW	1.98	2.82	2.98	3.19	–	–	
Relaxed with optB86b-vdW	PBE	1.92	2.76	2.94	3.15	2.41	2.59	(M)
	optB86b-vdW	2.00	2.84	2.99	3.20	–	–	
Experiment	PBE	1.96	2.79	2.99	3.21	2.44	2.63	(M)
	optB86b-vdW	2.04	2.89	3.05	3.27	–	–	

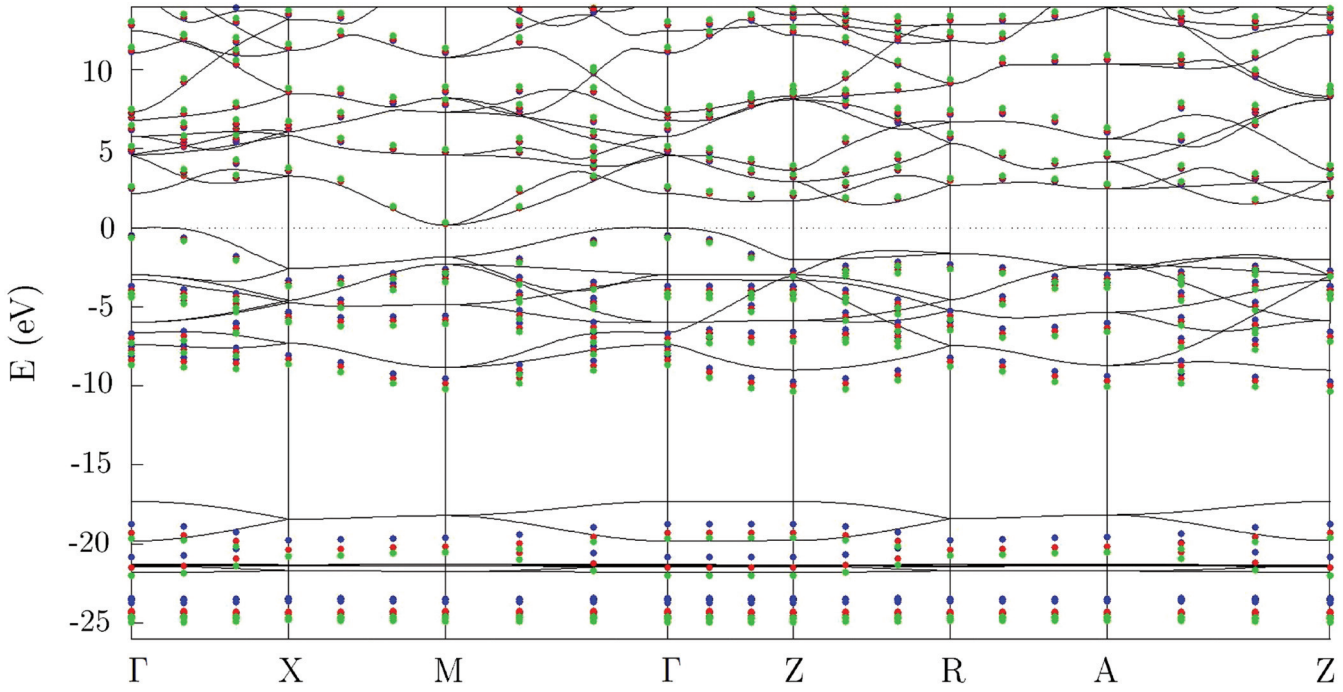

FIG. 4. (Color online) PBE band structure (full black lines), G_0W_0 (red dots), GW_0 (blue dots), and GW (green dots) results for lattice parameters and atomic positions obtained from the optB86b-vdW functional.

band gap found in Ref. 43 is considerably larger than the present PBE value of 0.04 eV. The difference in starting point (i.e., using the vdW eigenvalues and eigenfunctions or the bare PBE ones) observed for the PBE results is also reflected in the GW calculations. The GW_0 result for the experimental structure yields a value of 0.71 eV with the PBE Kohn-Sham eigenfunctions and is in excellent agreement with the experimental value of 0.7 eV, whereas using the optB86b-vdW eigenfunctions gives a somewhat larger value of 0.78 eV. The results of Table II show that an accurate value for the band gap can be obtained without relying on any experimental structural information or empirical input parameters. The GW_0 value for the structure optimized with optB86b-vdW is 0.75 eV when using the PBE eigenfunctions, which is somewhat larger than the experimental value.

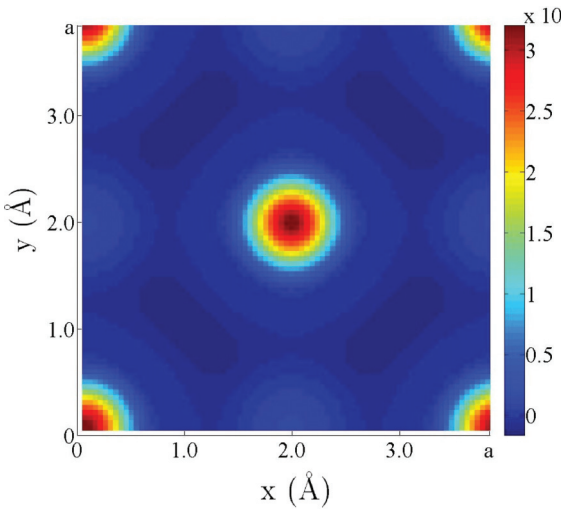

FIG. 5. (Color online) Charge density difference in the (001) plane containing the O atoms.

For larger systems GW calculations are often prohibited and hybrid functionals often provide a viable alternative. Therefore, for comparison, we have calculated the band gap with the popular HSE06 functional and its predecessor HSE03. When we use the structures optimized with the HSE functional (see Table I), a fundamental gap of 0.59 and 0.43 eV was found for HSE06 and HSE03, respectively. Since the hybrid functionals overestimate the volume (by ∼2.5%) it is expected that the value of the band gap will further decrease for the experimental lattice parameters and those optimized with the optB86b-vdW DF. This is shown in the last two columns of Table II, where, in line with the bare PBE and GW results, the same dependence of the calculated indirect band gap on the lattice parameters is observed.

Since optical experiments mainly probe the direct band gap we provide in Table III the direct gap of SnO, which is experimentally measured to be 2.7 eV. For the structure optimized without vdW forces, this gap is located at the Γ point, while for the experimental lattice parameters and the vdW-relaxed structure, the band gap is located at the M point. This result was also found in Ref. 19 and is a consequence of a lowering in energy of the conduction band minimum (at the M point) relative to the rest of the band, when the lattice parameters are optimized with the vdW functional. From Table III it follows that bare PBE underestimates the direct band gap, whereas the fully self-consistent GW with values ranging between 3.15 and 3.27 eV systematically overestimates the optical band gap. The best results are obtained with G_0W_0 and GW_0 that slightly overestimate the band gap. This small overestimation of the direct gap could

be a consequence of neglecting excitonic effects. In contrast to the results for the indirect band gap, the optimization of the structure with vdW-corrected functionals hardly changes the results for the direct band gap. For example a result of 1.93 eV is obtained for the structure optimized with PBE and with PBE eigenfunctions and 1.92 eV is found for its counterpart relaxed with the optB86b-vdW functional. However, it should be noticed that the values for relaxed with PBE correspond to the direct band gap at the Γ point, whereas the results for relaxed with optB86b-vdW correspond to the M point.

For structures optimized with HSE06 and HSE03, these functionals give a direct gap of 2.67 and 2.51 eV, respectively, at the Γ point, which is very close to the experimental value. The last two columns of Table III show the values of the direct band gap calculated with hybrid functionals for different optimized structures and the experimental lattice parameters. For all cases the values are very close to the experimental value of 2.7 eV, especially for the calculations with HSE06.

In Fig. 4 we present the band structure with eigenvalues obtained from the vdW-corrected PBE functional using the vdW-optimized structure (the other structures yield similar results). The GW eigenvalues are superimposed on the DFT band structure for several k points. The different colors of the points refer to the different levels of self-consistency of the GW calculations. While the conduction band minimum is hardly altered in going from the DFT to the quasiparticle approach, the valence band maximum exhibits a small decrease thereby opening the gap. For lower lying valence bands the GW results show a larger decrease in energy and the effect is stronger on increasing the level of self-consistency ($G_0W_0 \mapsto GW_0 \mapsto GW$). In particular, we find a downward shift of the Sn-d band by ∼3 eV with GW_0. Higher lying conduction bands show an increase in energy in comparison with the DFT-PBE results and the effect is stronger with the increasing level of self-consistency.

C. The nature of the van der Waals bond

In order to gain insight into the effect of the vdW functional on the interatomic bonding, we consider the charge density

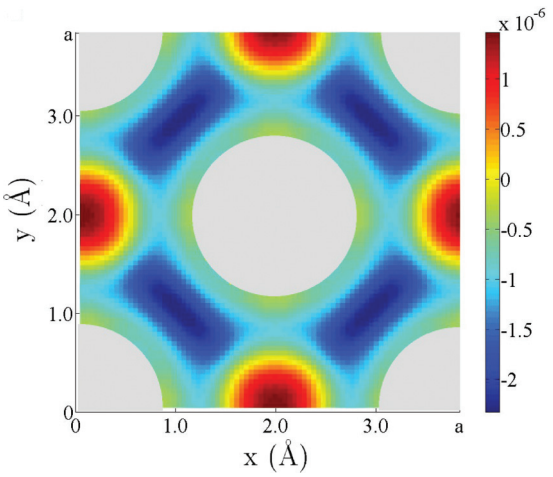

FIG. 6. (Color online) Charge density difference in the O plane, where the O atoms are artificially removed (gray areas).

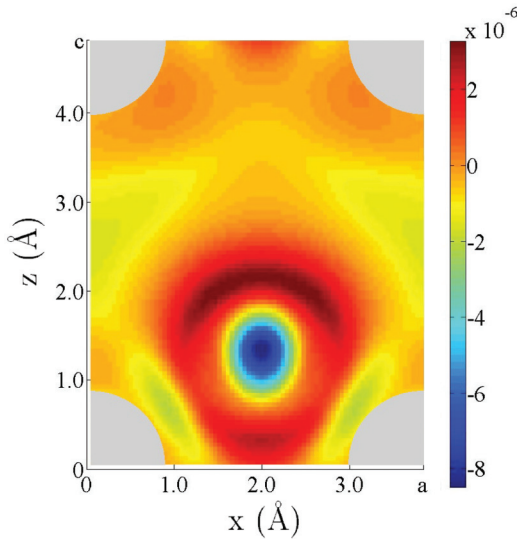

FIG. 7. (Color online) Charge density difference in the (010) plane, where the O atoms are artificially removed (gray areas).

difference,

$$\Delta\rho(\vec{r}) = \rho_{\mathrm{vdW}}(\vec{r}) - \rho_{\mathrm{novdW}}(\vec{r}),$$

where ρ_{vdW} is the charge density calculated with the optB86b-vdW DF and ρ_{novdW} is the density calculated with the same exchange part and local correlation part (LDA) but without the nonlocal contribution. In Fig. 5 we show $\Delta\rho$ for the (001) plane, containing the two O atoms. A relative large and almost spherical symmetric excess of electrons is observed in a narrow region around the O atoms when including the nonlocal contribution.

To visualize better the small changes in $\Delta\rho$ in between the O atoms, we artificially put the charge density around the O atoms to zero. For the (001) plane through the O atoms, this is shown in Fig. 6, where a depletion of electrons between the different O atoms is observed due to the vdW effect. There is also an excess of electron charge density between equivalent O atoms, coming from the Sn atoms, situated above and below the O plane. In Fig. 7 $\Delta\rho$ is shown for the (010) plane, containing a Sn atom and an O atom. Here again we artificially put the charge density around the O atoms to zero for visualization purposes. Due to the nonlocal contribution, the electron density around the Sn nuclei moves primarily to the region in between the Sn atoms along the c axis, and secondly to the region in between the Sn atom and the O plane. This charge redistribution due to the vdW contribution goes together with the observed reduction in the c parameter discussed in Sec. III A.

IV. CONCLUSION

In this work we have shown that a combination of current vdW-corrected functionals and state-of-the-art many-body calculations within the GW approximation provide accurate values for both structural and electronic properties without the need of experimental input or any empirical parameters. Together with the Grimme correction on PBE the optB86b-vdW functional accounts correctly for the vdW forces between

adjacent Sn layers. Subsequently this structure was used as input for the quasiparticle band structure calculations. We considered three levels of self-consistency for the GW calculations with G_0W_0 and GW_0 yielding results in close agreement with experiment (with slightly larger values for the latter) for both the fundamental and optical band gap and with the self-consistent GW overestimating both band gaps. Furthermore, we have investigated the effect of the structural details (lattice parameters and atomic positions) on the band gap demonstrating clearly the artificial opening of the gap when the structure is optimized with a non-vdW corrected functional. Moreover, we have shown that the Kohn-Sham eigenvalues and eigenfunctions which are used as starting point for the GW calculations affect the final value of the band gap: Using the vdW-corrected functional leads to a small increase of the band gap in comparison to the non-vdW corrected bare PBE functional. A detailed analysis of the interatomic bonding has shown that the vdW contribution results in relative large electron excess in a narrow region around the O atoms and a small depletion of electrons around the Sn atoms and between the O atoms.

ACKNOWLEDGMENTS

We gratefully acknowledge financial support from the IWT-Vlaanderen through the ISIMADE project, the FWO-Vlaanderen through project G.0150.13. K.G. thanks the University of Antwerp for a PhD fellowship. This work was carried out using the HPC infrastructure at the University of Antwerp (CalcUA), a division of the Flemish Supercomputer Center VSC, supported financially by the Hercules foundation and the Flemish Government (EWI Department).

*kirsten.govaerts@ua.ac.be

[1] S. Franz, G. Kent, and R. L. Anderson, J. Electron Mater. **6**, 107 (1977).
[2] M. Batzill and U. Diebold, Prog. Surf. Sci. **79**, 47 (2005).
[3] E. Fortunato, D. Ginley, H. Hosono, and D. C. Paine, Mater. Res. Bull. **32**, 242 (2007).
[4] W. Göpel and K. D. Schierbaum, Sensor Actuat. B **26**, 1 (1995).
[5] Z. Han, N. Guo, F. Li, W. Zhang, H. Zhao, and Y. Qian, Mater. Lett. **48**, 99 (2001).
[6] Y. Idota, T. Kubota, A. Matsufuji, Y. Mackawa, and T. Miyasaka, Science **176**, 1395 (1997).
[7] Y. Ogo, H. Hiramatsu, K. Nomura, H. Yanagi, T. Kamiya, M. Hirano, and H. Hosono, Appl. Phys. Lett. **93**, 032113 (2008).
[8] H. Hosono, Y. Ogo, H. Yanagi, and T. Kamiya, Electrochem. Solid-State Lett. **14**, H13 (2011).
[9] J. Pannetier and G. Denes, Acta Crystallogr. Sect. B **36**, 2763 (1980).
[10] G. W. Watson, J. Chem. Phys. **114**, 758 (2001).
[11] A. Walsh and G. W. Watson, Phys. Rev. B **70**, 235114 (2004).
[12] A. Walsh, D. J. Payne, R. G. Egdell, and G. W. Watson, Chem. Soc. Rev. **40**, 4455 (2011).
[13] A. Walsh and G. W. Watson, J. Phys. Chem. B **109**, 18868 (2005).
[14] O. Madelung, W. Von der Osten, and U. Rössler, *LB New Series: Intrinsic Properties of Group IV Elements and III-V, II-VI and I-VII* (Springer, Berlin, 1987).
[15] E. L. Peltzery Blancá, A. Svane, N. E. Christensen, C. O. Rodríguez, O. M. Cappannini, and M. S. Moreno, Phys. Rev. B **48**, 15712 (1993).
[16] I. Lefebvre, M. A. Szymanski, J. Olivier-Fourcade, and J. C. Jumas, Phys. Rev. B **58**, 1896 (1998).
[17] J. Raulot, G. Baldinozzi, R. Seshadri, and P. Cortona, Solid State Sci. **4**, 467 (2002).
[18] Y. Duan, Phys. Rev. B **77**, 045332 (2008).
[19] J. P. Allen, D. O. Scanlon, S. C. Parker, and G. W. Watson, J. Phys. Chem. C **115**, 19916 (2011).
[20] Q. Liu, Z. Liu, and L. Feng, Comp. Mater. Sci. **47**, 1016 (2010).
[21] L. A. Errico, Physica B **389**, 140 (2007).
[22] N. E. Christensen, A. Svane, and E. L. Peltzery Blancá, Phys. Rev. B **72**, 014109 (2005).
[23] R. W. Godby, M. Schlüter, and L. J. Sham, Phys. Rev. Lett. **56**, 2415 (1986).
[24] M. Dion, H. Rydberg, E. Schröder, D. C. Langreth, and B. I. Lundqvist, Phys. Rev. Lett. **92**, 246401 (2004).
[25] G. Román-Pérez and J. M. Soler, Phys. Rev. Lett. **103**, 096102 (2009).
[26] T. Thonhauser, V. R. Cooper, S. Li, A. Puzder, P. Hyldgaard, and D. C. Langreth, Phys. Rev. B **76**, 125112 (2007).
[27] J. Klimeš, D. R. Bowler, and A. Michaelides, Phys. Rev. B **83**, 195131 (2011).
[28] L. Hedin, Phys. Rev. **139**, A796 (1965).
[29] M. Shishkin and G. Kresse, Phys. Rev. B **74**, 035101 (2006).
[30] M. Shishkin and G. Kresse, Phys. Rev. B **75**, 235102 (2007).
[31] G. Kresse and J. Furthmüller, Comput. Mater. Sci. **6**, 15 (1996).
[32] G. Kresse and J. Furthmüller, Phys. Rev. B **54**, 11169 (1996).
[33] J. Heyd, G. E. Scuseria, and M. Ernzerhof, J. Chem. Phys. **118**, 8207 (2003).
[34] J. Heyd and G. E. Scuseria, J. Chem. Phys. **120**, 7274 (2004).
[35] J. Heyd and G. E. Scuseria, J. Chem. Phys. **121**, 1187 (2004).
[36] J. Heyd, J. E. Peralta, G. E. Scuseria, and R. L. Martin, J. Chem. Phys. **123**, 174101 (2005).
[37] A. V. Krukau, O. A. Vydrov, A. F. Izmaylov, and G. E. Scuseria, J. Chem. Phys. **125**, 224106 (2006).
[38] J. P. Perdew, K. Burke, and M. Ernzerhof, Phys. Rev. Lett. **77**, 3865 (1996).
[39] K. Lee, É. D. Murray, L. Kong, B. I. Lundqvist, and D. C. Langreth, Phys. Rev. B **82**, 081101 (2010).
[40] S. Grimme, J. Comput. Chem. **27**, 1787 (2006).
[41] K. Govaerts, M. H. F. Sluiter, B. Partoens, and D. Lamoen, Phys. Rev. B **85**, 144114 (2012).
[42] A. Togo, F. Oba, I. Tanaka, and K. Tatsumi, Phys. Rev. B **74**, 195128 (2006).
[43] D. Waroquiers, A. Lherbier, A. Miglio, M. Stankovski, S. Poncé, M. J. T. Oliveira, M. Giantomassi, G.-M. Rignanese, and X. Gonze, Phys. Rev. B **87**, 075121 (2013).